

2001-01-01

Eddies Induced in Cylindrical Containers by a Rotating End Wall

Christopher Hills

Technological University Dublin, chris.hills@dit.ie

Follow this and additional works at: <https://arrow.tudublin.ie/scschmatart>



Part of the [Applied Mathematics Commons](#), [Applied Mechanics Commons](#), [Fluid Dynamics Commons](#), and the [Mathematics Commons](#)

Recommended Citation

Hill, C. P.: Eddies Induced in Clindrical Containers by a Rotating End Wall, *Physics of Fluids*, 2001, Vol.13, issue 1, pp.2279-2286. doi.org/10.21427/2d60-br42

This Article is brought to you for free and open access by the School of Mathematics at ARROW@TU Dublin. It has been accepted for inclusion in Articles by an authorized administrator of ARROW@TU Dublin. For more information, please contact arrow.admin@tudublin.ie, aisling.coyne@tudublin.ie.



This work is licensed under a [Creative Commons Attribution-Noncommercial-Share Alike 4.0 License](#)

Eddies induced in cylindrical containers by a rotating end wall

Christopher P. Hills^{a)}

Lincoln College, Oxford OX1 3DR, England

(Received 12 July 2000; accepted 23 April 2001)

The flow generated in a viscous liquid contained in a cylindrical geometry by a rotating end wall is considered. Recent numerical and experimental work has established several distinct phases of the motion when fluid inertia plays a significant role. The current paper, however, establishes the nature of the flow in the thus far neglected low Reynolds number regime. Explicitly, by employing biorthogonality relations appropriate to the current geometry, it is shown that a sequence of exponentially decaying eddies extends outward from the rotating end wall. The cellular structure is a manifestation of the dominance of complex eigensolutions to the homogeneous problem and arises as the result of nonlinear forcing associated with an inertial correction to the Stokes flow. © 2001 American Institute of Physics. [DOI: 10.1063/1.1384470]

I. INTRODUCTION

We consider an incompressible, Newtonian viscous fluid, contained within a semi-infinite circular cylinder, and study the low Reynolds number flow produced by the steady rotation of an end wall (see Fig. 1). Recently there has been considerable experimental interest in this geometry, but the focus has been largely on a range of Reynolds numbers, Re , in which the fluid inertia plays a significant role. Vogel¹ showed that, as a stability bound is reached, the base flow, consisting of a large toroidal vortex that flows up the outer cylinder boundary to return down a small central core,² generates a region of recirculation on the axis of symmetry.³ The stability limit is defined by a curve lying in the plane of aspect ratio versus Reynolds number. Vogel was the first to draw parallels between the “bubble” creation and the problem of vortex breakdown. The possible link is undoubtedly intriguing and has motivated several papers. In particular, Brøns, Voigt, and Sørensen⁴ discussed the question of vortex breakdown for the current geometry using a combination of bifurcation theory and numerical simulations. Earlier, Escudier⁵ verified the Vogel curve and extended the stability diagram to a wider range of aspect ratios and Reynolds numbers. That work not only identified the stability curves of two further breakdowns, each with an associated “bubble,” but also revealed subsequent transitions to oscillatory and turbulent regimes. The oscillatory, time-dependent states of the geometry have been further studied, both experimentally and numerically, by Stevens, Lopez, and Cantwell.⁶ More recently, the work of Mullin, Kobine, Tavener, and Cliffe,⁷ while confirming the known results for a single cylinder, gives an important insight into the influence of the geometry. Explicitly these authors have considered a configuration in which a coaxial central column is introduced with the possibility of differential rotation. The inner column was taken as (i) a circular cylinder and (ii) the frustum of a right circular

cone. In the latter case they provided complementary experimental and numerical work, showing that, when the cross section increased vertically away from the end boundary, the recirculating “bubble” was reinforced, but that a tapering column suppressed the onset of the new region.

In this paper we concentrate on low Reynolds number flow in a single cylinder, a regime that has been somewhat overlooked, although it is likely to give valuable insight into general flow structures. We find that, as a result of a first-order inertial correction, toroidal eddies appear. Previously, toroidal eddies have been predicted even in an inertialess (Stokes) regime of a cylindrical geometry, but with physical driving mechanisms somewhat different from our present concern. For example, Fitz-Gerald⁸ modeled the Stokes flow of a plasma contained between two red blood cells moving with uniform velocity within a narrow capillary. The author found that the expected Poiseuille flow is modified by a complex eigenfunction contribution introduced to accommodate the boundary conditions on the end blood cells. By a numerical analysis, Fitz-Gerald⁸ showed that the combined solution could generate small secondary circulations within the plasma. Also, with an aim of modeling the fluid motion due to cilia, Liron and Shahar⁹ considered the motion generated by Stokeslets (represented by delta function forcing) in an infinite circular cylinder. Their flow solution exploited the linearity of the Stokes equations and combined the Happel and Brenner¹⁰ series solution of the homogeneous problem with a particular solution for the singular forcing (not necessarily placed on the axis of symmetry). Liron and Shahar⁹ did consider in some detail the case when the Stokeslet does lie on the axis of symmetry, resolving the problem by numerical means. Later, Blake¹¹ extended their work by discussing toroidal eddies produced in infinite, semi-infinite, and finite cylinders when the Stokeslet lies on the axis of symmetry. He constructed his solution using the superposition of eigenfunctions to the homogeneous Stokes problem in the cylindrical geometry. The associated eigenvalues are complex and lead directly to toroidal eddies. Blake¹¹ produced numerical visualizations by either calculating series

^{a)}Telephone: +44 1865 288090; fax: +44 1865 279802; electronic mail: chris.hills@lincoln.ox.ac.uk

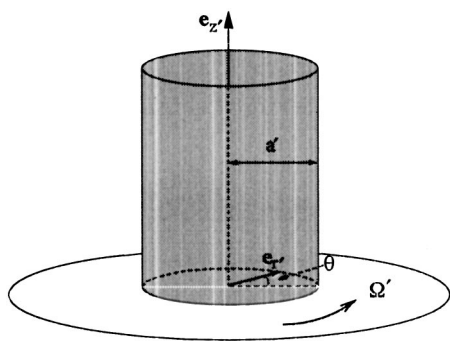


FIG. 1. Geometry of the single semi-infinite circular cylinder of radius a' with a rotating end wall, of angular velocity Ω' about the axis of symmetry, relative to a cylindrical polar coordinate system (r', θ, z') .

constants using a least squares criterion or using a finite difference scheme over the domain.

The driving force of the cylinder flow investigated here is a rotating lower plate. This configuration has the obvious advantage of being easily amenable to experimental investigation. We are concerned with the low Reynolds number regime and proceed in Sec. II to construct an asymptotic series in terms of Re for the velocity and pressure fields. On physical grounds we look for a solution in which there is exponential decay in the perpendicular (z) direction away from the plate. The zeroth-order flow is purely azimuthal, given by a series involving orthogonal Bessel functions whose coefficients are determined in an obvious fashion. Heuristically we expect the first-order correction due to inertia to be toroidal and two-dimensional and it can, therefore, be expressed in terms of a streamfunction. This function satisfies a fourth-order forced differential equation involving a well-known second-order cylindrical differential operator¹² $\{\mathcal{D}^2\}$. The exponentially z -decaying solution is found as a combination of a particular solution (relating to the forcing induced by the Stokes solution) and a complementary solution that will ensure that the homogeneous boundary condition of the combined solution is satisfied on the rotating end wall. Both the particular and complementary solutions are found as an infinite series. The boundary condition on the side wall is imposed on each individual term of each series. The complementary solution leads to an eigenvalue problem that is characteristic of the geometry and the second-order cylindrical differential operator, \mathcal{D}^2 , which occurs frequently in studies of cylinder flows. That the eigenvalues are complex is known¹³ from, for example, the work of Blake¹¹ and, associated with these eigenvalues, there is a toroidal eddy structure. The fundamental consideration is whether the particular or the complementary solution dominates.

The competition between particular and complementary solutions is an important feature of the investigations of Moffatt¹⁵ and Moffatt and Duffy¹⁶ relating to a wedge geometry. These authors have established that geometry can have a deciding role. By varying the boundary configuration they show that the relative dominance of particular solutions and local similarity solutions can swap over. It is this interchange of dominance that alters the flow character. In particular, for wedge geometries that include a "corner," the appearance of

the eddies described by Moffatt¹⁷ is fundamentally dependent on the corner angle: the internal angle of the wedge determines not only if eddies appear but also the asymptotic radial power as the corner is approached, the intensity of the eddies and the extent to which they penetrate the corner (see Hills¹⁸). Although in the classic two-dimensional, linear, Taylor¹⁹ scraping problem eddies never appear, Hills and Moffatt²⁰ show that the extension of the geometry to three dimensions allows the presence of eddies for a range of corner angles. In Sec. II we show that, for the geometry associated with a cylinder with a rotating end wall, the leading complex eigenvalue of the homogeneous problem dominates all other toroidal terms and indicates the presence of eddies.

Our flow solution for the rotating end wall problem is based upon series expansions that require the determination of coefficients. The Stokes solution and the particular solution component of the toroidal streamfunction are in terms of orthogonal functions and their series resolution present no great difficulties. However, the complementary functions are not orthogonal and the determination of their coefficients so as to satisfy an inhomogeneous boundary condition is less straightforward. Liron and Shahar⁹ and Blake¹¹ rely on numerical methods of approximation and truncation. In this work we seek to employ appropriate biorthogonality relations but we need to demonstrate that the solution scheme outlined in Sec. II is indeed self-consistent. Accordingly, in Sec. III we demonstrate that the method of Smith,²¹ later developed by Joseph²² and co-workers (see Joseph and Sturges,²³ Joseph, Sturges, and Warner,²⁴ Liu and Joseph²⁵), can be extended and used in respect of the eigenfunctions of the operator \mathcal{D}^4 so yielding an analytical method of determining a series solution. The method, however, has to be exercised with caution. Spence²⁶ and Harper and Wake²⁷ considered the Cartesian description of the flow in a rectangle open at one end with prescribed data on the opposite boundary and demonstrated that such solutions can be unstable with respect to the order of truncation so compromising convergence within the required domain. In the current work, once we have established the validity of the solution scheme, we do not explicitly determine the series constants nor do we explore questions of completeness or convergence but concentrate on identifying the dominant physical effects. We find that the mechanism of the cellular structure in our flow is essentially the same as in the higher Re case (see Ref. 2), but our analysis provides a quantitative measure (given by the periodicity of the streamfunction) that is capable of being tested experimentally.

II. THE FORMATION OF EDDY CELLS IN A "SCRAPING" CYLINDER

A. Problem description and formulation

We consider a vertical, hollow, circular cylinder of radius a' , held stationary, in scraping contact²⁸ with a horizontal plane rotating with constant angular speed Ω' about the axis of the cylinder (see Fig. 1). The cylinder is filled with an incompressible, viscous fluid of constant kinematic viscosity ν' that is assumed to be in steady motion, driven by the rotation of the bottom plate. The velocity, $\mathbf{u}=(u,v,w)$, and

pressure, p' , fields will be determined by the solutions of the steady Navier–Stokes equations subject to the usual no-slip boundary conditions on the cylinder walls and end plate. In addition, we shall impose a decay constraint ensuring that \mathbf{u} must vanish at large distances from the rotating plate. We use the obvious length scale, a' , and typical speed, $\Omega'a'$, to nondimensionalize our problem. Specifically, we set

$$r=r'/a', \quad z=z'/a', \quad \mathbf{u}=\mathbf{u}'/\Omega'a', \quad p=p'/\nu'\Omega', \tag{1}$$

where (r', θ, z') are the usual cylindrical polar coordinates shown in Fig. 1 and the Reynolds number of the flow, Re , is given by

$$\text{Re}=\Omega'a'^2/\nu'. \tag{2}$$

In terms of these new variables, the system is governed by

$$\begin{aligned} \nabla \cdot \mathbf{u} &= 0, \\ \text{Re}(\mathbf{u} \cdot \nabla)\mathbf{u} &= -\nabla p + \nabla^2 \mathbf{u}, \end{aligned} \tag{3}$$

with boundary conditions

$$\begin{aligned} u=v=w &= 0, \quad \text{on } r=1, \\ u=w &= 0, \quad v=r, \quad \text{on } z=0, \\ u,v,w &\rightarrow 0, \quad \text{as } z \rightarrow \infty. \end{aligned} \tag{4}$$

The intrinsic geometrical symmetry and the boundary conditions lead us to look for axisymmetric solutions (so that $\partial/\partial\theta \equiv 0$) with the pressure and velocity fields functions of r and z only but with the z dependence exponentially decaying.

Our analysis is concerned with the low Reynolds number regime and we shall construct asymptotic power series expansions in Re . Specifically, if χ denotes either \mathbf{u} or p , we assume

$$\chi = \chi_0 + \text{Re} \chi_1 + \text{Re}^2 \chi_2 + \dots \tag{5}$$

By substituting these expansions into (3) and equating powers of Re , we generate the following system for determining the successive pairs $\{\mathbf{u}_n, p_n\}$,

$$\begin{aligned} \nabla \cdot \mathbf{u}_n &= 0, \\ \sum_{k=0}^{n-1} (\mathbf{u}_k \cdot \nabla)\mathbf{u}_{n-1-k} &= -\nabla p_n + \nabla^2 \mathbf{u}_n, \quad n \geq 1. \end{aligned} \tag{6}$$

From (6) we see that the underlying equations for each pair $\{\mathbf{u}_n, p_n\}$ are linear, and so a uniformly valid solution may be constructed as the sum of an inhomogeneous part (due to lower-order forcing) and a complementary solution related to the homogeneous problem. It will be essential to assess the relative dominance of these two contributions.

B. The solution to Stokes flow equations

From (6) we see that, at the zeroth order the velocity and pressure fields $\{(u_0, v_0, w_0), p_0\}$ satisfy Stokes flow equations. The boundary conditions (4) suggest a purely azimuthal velocity profile so we set $u_0 = w_0 = 0$ and find that the radial and vertical components of the governing equations imply a constant pressure, i.e., $p_0(r, z) = \text{const}$. The azimuthal velocity component satisfies

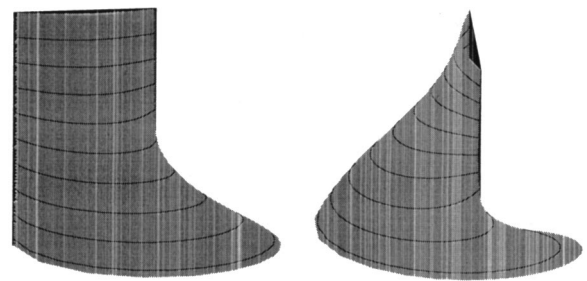


FIG. 2. The Stokes flow generated by a cylinder scraping over a rotating plate. Two views of the displacement surface showing both the distance traveled in a fixed time by particles initially on the plane $\theta=0$ (indicated in black) and the exponential decay in the z direction.

$$\frac{\partial^2 v_0}{\partial r^2} + \frac{1}{r} \frac{\partial v_0}{\partial r} - \frac{1}{r^2} v_0 + \frac{\partial^2 v_0}{\partial z^2} = 0. \tag{7}$$

We look for a series solution employing a separation of variables. On physical grounds we expect spatial decay in the z direction and so assume

$$v_0(r, z) = \sum_{k=1}^{\infty} v^k(r) e^{-\lambda_k z}. \tag{8}$$

The sequence $\{\lambda_k\}$ will be resolved later via an eigenvalue problem.

Substituting (8) into (7) we find that the $v^k(r)$ satisfy Bessel's equation of order one so that they can be expressed as linear combinations of the Bessel functions $J_1(\lambda_k r)$ and $Y_1(\lambda_k r)$. Our solution must be finite at $r=0$ so that $Y_1(\lambda_k r)$ cannot contribute. When we apply the boundary condition (4) on $r=1$ we find that the λ_k are zeros of J_1 and are, therefore, all real. To ensure our solutions properly decay we restrict attention to the positive roots. It is convenient to order the λ_k by magnitude so that, henceforth, $0 < \lambda_1 < \lambda_2 < \lambda_3$, etc. Thus, v_0 is given by

$$v_0(r, z) = \sum_{k=1}^{\infty} A_k J_1(\lambda_k r) e^{-\lambda_k z}, \quad \text{where } J_1(\lambda_k) = 0. \tag{9}$$

Using the orthogonality of Bessel functions and the boundary condition on $z=0$, the constants A_k are found to be

$$A_k = 2 \int_0^1 r^2 J_1(\lambda_k r) dr / J_1'(\lambda_k)^2 = -2/\lambda_k J_0(\lambda_k), \tag{10}$$

where J_0 is the Bessel function of the first kind of order zero. The zeros, λ_k , of J_1 are well known (see, for example, Abramovitch and Stegun²⁹) with the first three being

$$\lambda_1 = 3.832, \quad \lambda_2 = 7.016, \quad \lambda_3 = 10.173. \tag{11}$$

We find from (10) that

$$A_1 = 1.296, \quad A_2 = -0.950, \quad A_3 = 0.787.$$

Figure 2 shows, from two viewpoints, the distance traveled in a fixed time by particles originating on the plane $\theta=0$. The Stokes flow is purely azimuthal so particles move in a circular fashion about the vertical axis of symmetry, but

the speed of particles decays exponentially as we move away from the driving plate. As z increases, the dominant flow contribution is given by

$$1.296 J_1(3.832r)e^{-3.832z},$$

so that, in essence, the azimuthal flow may be thought of as being substantially contained within a thin z layer. Outside the layer the fluid velocities are very small. (For example, for $z > 0.35$ the maximum nondimensional azimuthal velocity is always less than 0.2.)

C. The first-order Re correction

From Eq. (6), the first-order corrections for the velocity and pressure fields satisfy

$$\begin{aligned} \nabla \cdot \mathbf{u}_1 &= 0, \\ -\nabla p_1 + \nabla^2 \mathbf{u}_1 &= \mathbf{u}_0 \cdot \nabla \mathbf{u}_0, \end{aligned} \tag{12}$$

together with the homogeneous set of boundary conditions for \mathbf{u}_1 , viz.

$$\begin{aligned} \mathbf{u}_1 &= \mathbf{0}, \quad \text{on } z=0 \quad \text{and } r=1, \\ \mathbf{u}_1 &\rightarrow \mathbf{0}, \quad \text{as } z \rightarrow \infty. \end{aligned}$$

Since the zeroth-order velocity is purely azimuthal, the forcing represented by the right-hand side of (12b) lies in the (r, z) plane. Most importantly, since the zeroth-order solution has no radial or axial velocity components, the first-order terms in these directions will have a defining role on the flow character. We assume that the first-order motion is in the (r, z) plane and seek a steady axisymmetric solution. We may eliminate the pressure field in the usual manner to obtain the vorticity equation

$$\nabla^2(\nabla \times \mathbf{u}_1) = -2v_0 r^{-1} \partial v_0 / \partial z \mathbf{e}_\theta. \tag{13}$$

But, since \mathbf{u}_1 is solenoidal and two-dimensional, it is appropriate to introduce a streamfunction, ψ , by

$$\mathbf{u}_1 = \nabla \times [0, r^{-1} \psi(r, z), 0] = r^{-1} (-\partial \psi / \partial z, 0, \partial \psi / \partial r), \tag{14}$$

and we are led to

$$\mathcal{D}^2(\mathcal{D}^2 \psi) = 2v_0 \partial v_0 / \partial z, \tag{15}$$

where the operator \mathcal{D}^2 is given by (see Ref. 12)

$$\mathcal{D}^2 \equiv \frac{\partial^2}{\partial z^2} + r \frac{\partial}{\partial r} \left(\frac{1}{r} \frac{\partial}{\partial r} \right). \tag{16}$$

In terms of ψ , the homogeneous boundary conditions give

$$\partial \psi / \partial z = \partial \psi / \partial r = 0, \quad \text{on } r=1 \quad \text{and } z=0. \tag{17}$$

Equations (15)–(17) constitute a biharmonic system under specific forcing with homogeneous boundary conditions. We construct a general solution as the sum of a particular solution, ψ^P , to the forced problem and a complementary solution, ψ^C (with no applied forcing).

Let us first consider the forced problem. Substituting the series solution of (9) into (15), we find

$$\mathcal{D}^4 \psi^P = 2 \sum_{l=1}^{\infty} \sum_{m=1}^{\infty} \lambda_l A_l A_m J_1(\lambda_l r) J_1(\lambda_m r) e^{-(\lambda_l + \lambda_m)z}, \tag{18}$$

where the $\{A_k\}$ are determined by (10) and the $\{\lambda_k\}$ are the ordered sequence of positive roots of J_1 . In order to accommodate the z dependence of the forcing, we assume

$$\psi^P = \sum_{l=1}^{\infty} \sum_{m=1}^{\infty} \Psi_{lm}^P(r) e^{-(\lambda_l + \lambda_m)z}. \tag{19}$$

From (18), the function Ψ_{lm}^P satisfies the ordinary differential equation

$$\begin{aligned} \left(\frac{d^2}{dr^2} - \frac{1}{r} \frac{d}{dr} + (\lambda_l + \lambda_m)^2 \right)^2 \Psi_{lm}^P \\ = 2\lambda_l A_l A_m J_1(\lambda_l r) J_1(\lambda_m r). \end{aligned} \tag{20}$$

While the decomposition of (19) is not unique (as the functions Ψ_{lm}^P and Ψ_{ml}^P have the same exponential z dependence), Eq. (20) removes any ambiguity and, following from the assumed linear independence of the exponential functions, we obtain a series of independent differential equations. Using the tabulated zeros λ_k , the solution for each Ψ_{lm}^P can be constructed as a (complete) series in Bessel functions of the first kind, viz.,

$$\begin{aligned} \Psi_{lm}^P = a_{lm}^0 + \sum_{n=1}^{\infty} a_{lm}^n r J_1(\lambda_n r) + A_{lm} r J_1[(\lambda_l + \lambda_m) r] \\ + B_{lm} r^2 J_0[(\lambda_l + \lambda_m) r]. \end{aligned} \tag{21}$$

When we substitute (21) onto the left-hand side of (20), we find

$$(\lambda_l + \lambda_m)^4 a_{lm}^0 + \sum_{n=1}^{\infty} a_{lm}^n r J_1(\lambda_n r) [(\lambda_l + \lambda_m)^2 - \lambda_n^2]^2. \tag{22}$$

Thus, each $\{a_{lm}^n\}$ ($n=1,2,\dots$) is determined using the orthogonality of Bessel functions by multiplying (20) by $J_1(\lambda_n r)$ and integrating over the range $[0, 1]$. [Note that, by evaluating (20) at $r=0$, we obtain $a_{lm}^0=0$.] The constants A_{lm} and B_{lm} are chosen to ensure that $\Psi_{lm}^P(1) = \Psi_{lm}^{P'}(1) = 0$. It is clear that, by this procedure, a particular solution can be found satisfying all boundary conditions, except those on $z=0$. Our primary interest is, however, with the dominant (r, z) -velocity components. As we move vertically away from the horizontal plate the dominant contribution to ψ^P comes from the term with smallest exponent (viz., $\Psi_{11}^P e^{-2\lambda_1 z}$) which, from (11a), has a decay rate of $2\lambda_1 \approx 7.6$. Therefore, as might be expected, the nonlinear term forces a particular solution that decays extremely rapidly.

The particular solution based on (21) will not generally satisfy the boundary conditions on the lower plate and to accommodate these conditions we introduce a complementary function, ψ^C , that will satisfy the unforced biharmonic equation and have zero partial derivatives on the cylinder $r=1$. The behavior for large z suggests a series

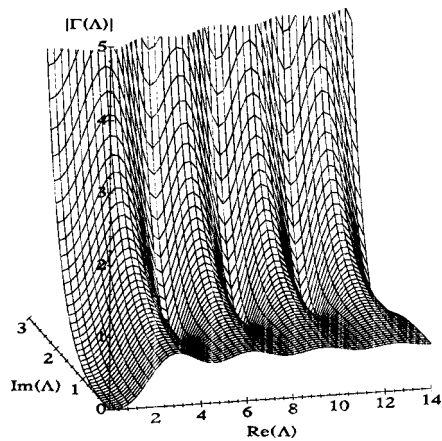


FIG. 3. The absolute value of the function $\Gamma(\Lambda)$ of (25). The roots occur at the minima of the function, which can be seen as a sequence of troughs on the surface.

$$\psi^C = \sum_{k=1}^{\infty} \Psi_k^C(r) e^{-\Lambda_k z}, \tag{23}$$

and we find that, by taking³⁰

$$\begin{aligned} \Psi_k^C = & [\mathcal{A}_k r^2 J_0(\Lambda_k r) + \mathcal{B}_k r J_1(\Lambda_k r) + \mathcal{C}_k r^2 Y_0(\Lambda_k r) \\ & + \mathcal{D}_k r Y_1(\Lambda_k r)], \end{aligned} \tag{24}$$

we can satisfy the biharmonic equation. To get a finite velocity field at $r=0$ we must discard the Bessel functions of the second kind (Y_0, Y_1), and to satisfy the conditions on $r=1$ we require

$$\Gamma(\Lambda_k) \equiv \Lambda_k J_1(\Lambda_k)^2 - 2J_0(\Lambda_k)J_1(\Lambda_k) + \Lambda_k J_0(\Lambda_k)^2 = 0, \tag{25}$$

and

$$\mathcal{A}_k = -\mathcal{B}_k J_1(\Lambda_k) / J_0(\Lambda_k). \tag{26}$$

Figure 3 shows a plot of the absolute value of $\Gamma(\Lambda)$ in the complex plane.³¹ There are no real roots of (25) so that the z -decay rates of the complementary function are given by the real part of complex roots. The first three complex roots (see Friedmann, Gillis, and Liron¹⁴), ordered by the positive real part (the solution must decay), are

$$\begin{aligned} \Lambda_1 &= 4.466\,30 + 1.467\,47i, & \Lambda_2 &= 7.694\,10 + 1.726\,97i, \\ \Lambda_3 &= 10.874\,58 + 1.894\,94i, & \dots \end{aligned}$$

Thus the complementary function is given by the series solution

$$\begin{aligned} \psi^C = \text{R} \left(\sum_{k=1}^{\infty} \tilde{\mathcal{B}}_k [J_0(\Lambda_k) r J_1(\Lambda_k r) \right. \\ \left. - J_1(\Lambda_k) r^2 J_0(\Lambda_k r)] e^{-\Lambda_k z} \right), \end{aligned} \tag{27}$$

where $\{\tilde{\mathcal{B}}_k\}$ are complex constants intended to adjust the particular solution ψ^P so that the composite solution has vanishing partial derivatives on $z=0$.

The important observation at this point is that the z -decay constant associated with $\Lambda_1 \sim 4.47$ (the leading-order

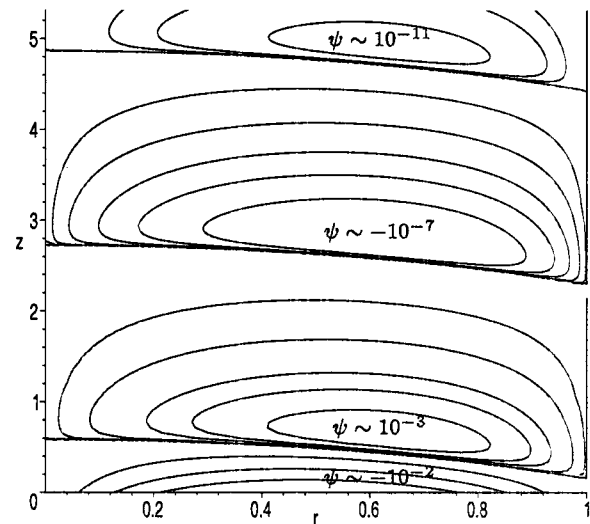


FIG. 4. A plot of the eddy structure attributable to the dominant, first-order complementary streamfunction $\text{R}[\Psi_1^C e^{-\Lambda_1 z}]$, illustrated using $\tilde{\mathcal{B}}_1=1$. Flow intensity is indicated by the contour values taken as $\psi = (0, -5 \times 10^{-2}, -2 \times 10^{-2}, -5 \times 10^{-3}, 2 \times 10^{-3}, 1 \times 10^{-3}, 5 \times 10^{-4}, 1 \times 10^{-4}, 1 \times 10^{-5}, -8 \times 10^{-8}, -3 \times 10^{-8}, -1 \times 10^{-8}, -2 \times 10^{-9}, -2 \times 10^{-10}, 1 \times 10^{-11}, 3 \times 10^{-12}, 1 \times 10^{-12})$.

term of ψ^C) is smaller than that arising from the dominant zeroth-order forcing (~ 7.6) of the particular solution ψ^P . Thus, as z increases the complementary function will dominate (assuming $\tilde{\mathcal{B}}_1 \neq 0$). Since Λ_1 is complex, a periodicity in the z direction will be present. The (r, z) motion will be dominated by a sequence of stacking spatially (z) decaying cells and is illustrated in Fig. 4 by a contour plot of $\text{R}[\Psi_1^C e^{-\Lambda_1 z}]$, with $\tilde{\mathcal{B}}_1$ notionally taken as unity. The periodicity of the cells will be governed by the imaginary part, i.e., $\Im(\Lambda_1)$. (Note that, for this function in isolation, the boundary conditions on $z=0$ are clearly not satisfied but they are satisfied on $r=1$.)

Our discussion has established that the solution for the scraping cylinder problem is dominated by a zeroth-order azimuthal flow. To first order, this azimuthal flow is modified by a cellular structure involving the radial and vertical velocity components. The series constants for the particular solution are immediately found using the orthogonality of Bessel functions. We note that the eigenvalues of the complementary solution are only dependent on the geometry and not on the primary flow. Therefore only the intensity, not the shape, of the cell-like structure is affected by v_0 in the form of the constants $\tilde{\mathcal{B}}_k$. Throughout our discussion of the dominant contribution to the solution we have tacitly assumed that the constants $\tilde{\mathcal{B}}_k$ are readily determinable without stating how this task is to be achieved. In the next section we develop a biorthogonality condition that will enable us to determine the $\tilde{\mathcal{B}}_k$'s and will essentially complete the arguments of the present section.

III. BIORTHOGONALITY RELATION FOR EIGENFUNCTIONS OF \mathcal{D}^4

In the previous section, by considering dominant effects we have established, in principle, the presence of toroidal

eddies in low Reynolds number flow. But we still need to establish that the series constants, \tilde{B}_k , for the complementary solution can indeed be found for given boundary conditions and, in addition, elucidate a practical method of determining them. Essentially we need an orthogonality condition between the complementary functions Ψ_k^C . In this section we provide such a biorthogonality condition for the solutions of our fourth-order operator \mathcal{D}^4 . The method we employ is substantially due to Smith,²¹ who established biorthogonality relations to solve the biharmonic equation governing the bending of a semi-infinite elastic strip that is clamped along its long edges with prescribed data on the short edge. These relations have been used in conjunction with Stokes equations in fluid dynamics by Joseph²² and his collaborators (see the following references). In most cases the prescribed boundary data is not canonical and results in an infinite set of coupled linear equations in an infinite number of unknowns. Usually the only practical way of dealing with such a set of coupled equations is to solve numerically a truncated set of equations for a finite number of coefficients. This approach was used by Joseph and Sturges²³ to demonstrate a stack of eddies for the Stokes flow generated in a rectangular cavity by a sliding plate along one edge. Khuri³² established (following the method of Liu and Joseph²⁵) a biorthogonality relation for a variation of the similarity solutions investigated by Moffatt.¹⁷ Khuri used numerical truncation to find the Stokes flow in a sector of a doughnut shape driven by a uniformly moving plate at one of the radial boundaries. However, in all these cases the provision of a biorthogonality relation ensures that a solution is possible and will provide an accurate method of determining the constants, even under truncation.

The convergence of an infinite series solution is, of course, important. Smith²¹ established convergence for his biorthogonal series of eigenfunctions of the biharmonic equation, but under somewhat severe conditions on the boundary data. Later Joseph,²² Joseph and Sturges,²³ and Joseph, Sturges, and Warner²⁴ were able to relax the sufficient conditions found by Smith. Without explicitly finding a solution, we do not attempt an analysis of the convergence conditions for our series. Our principal concern is to demonstrate that the determination of our series constants is possible. As pointed out by Smith,²¹ the divergence of the series of complementary functions on the prescribing boundary need not be catastrophic: the complementary functions are dominated by an exponential decay in the vertical coordinate, making the series asymptotic (and, therefore, useful) in this direction.

Let us now turn to the complementary solution given by (23). For notational clarity, we shall henceforth drop the superscript C and, in order to facilitate our analysis, the constants \tilde{B}_k will no longer be included in the definition of $\Psi_k(x)$ but will now appear explicitly in the series, modified by a factor of Λ_k^2 . Thus, relative to a cylindrical polar coordinate system, we have a series solution for the streamfunction satisfying $\mathcal{D}^4\psi=0$, in the domain $(r,z) \in [0,1] \times [0,\infty)$, given by

$$\psi = \sum_{k=1}^{\infty} \tilde{B}_k \Psi_k e^{-\Lambda_k z / \Lambda_k^2}. \tag{28}$$

The eigenfunctions $\Psi_k(r)$ satisfy homogeneous boundary conditions on $r=1$ and we require that, on the boundary $z=0$, the streamfunction ψ and its derivative should match the particular solution in order that their sum satisfy (17). To keep our discussion general we write

$$\partial\psi/\partial r = F(r), \quad \partial\psi/\partial z = G(r), \quad \text{on } z=0, \tag{29}$$

where F and G have to be regarded as known functions. The eigenfunctions Ψ_k are given by

$$\Psi_k = [J_0(\Lambda_k)rJ_1(\Lambda_k r) - J_1(\Lambda_k)r^2J_0(\Lambda_k r)], \tag{30}$$

and the eigenvalues Λ_k satisfy (25). We introduce a second eigenfunction $\hat{\Psi}_k$ with the ambition of reducing the fourth-order biharmonic equation to a pair of coupled second-order equations. We define

$$\hat{\Psi}_k = \frac{1}{\Lambda_k^2} r \frac{d}{dr} \left(\frac{1}{r} \frac{d}{dr} \right) \Psi_k = -\Psi_k + 2J_1(\Lambda_k)rJ_1(\Lambda_k r). \tag{31}$$

The governing equations become

$$\begin{aligned} \Psi_k'' - \Lambda_k^2 \hat{\Psi}_k &= 0, \\ \hat{\Psi}_k'' + \Lambda_k^2 (2\hat{\Psi}_k + \Psi_k) &= 0, \end{aligned} \tag{32}$$

where we have used " " to denote the operator $rd/dr[r^{-1}d/dr]$. The pair of equations (32) can be conveniently expressed in matrix form as

$$\Psi_k'' + \Lambda_k^2 \mathbf{M} \Psi_k = \mathbf{0}, \tag{33}$$

with

$$\mathbf{M} = \begin{pmatrix} 0 & -1 \\ 1 & 2 \end{pmatrix}, \quad \Psi_k = \begin{pmatrix} \Psi_k \\ \hat{\Psi}_k \end{pmatrix}. \tag{34}$$

To construct a biorthogonality condition we introduce the adjoint problem. The adjoint eigenfunctions $\Phi_k = (\Phi_k, \hat{\Phi}_k)^T$ satisfy

$$\Phi_k'' + \Lambda_k^2 \mathbf{M}^T \Phi_k = \mathbf{0}, \tag{35}$$

where the superscript "T" indicates the usual transpose. By eliminating Φ_k from (35), it is straightforward to show that $\hat{\Phi}_k$ satisfies the original fourth-order differential equation in r that arises when a separation of (r, z) variables is used on the biharmonic equation. Thus, we take

$$\hat{\Phi}_k = \Psi_k. \tag{36}$$

Then the second component of (35) yields an expression for Φ_k given by

$$\Phi_k = 2\hat{\Phi}_k + \hat{\Phi}_k'' / \Lambda_k^2 = 2\Psi_k + \hat{\Psi}_k. \tag{37}$$

We are now in a position to write down the biorthogonality relation. We define a binary operator $\langle \cdot, \cdot \rangle$ on functional vectors \mathbf{a}, \mathbf{b} by

$$\langle \mathbf{a}, \mathbf{b} \rangle = \int_0^1 \frac{1}{r} \mathbf{a}^T \mathbf{M} \mathbf{b} \, dr. \tag{38}$$

We will apply this binary relation to Ψ_n and its adjoint Φ_m , but first we must make explicit some boundary conditions. The homogeneous boundary conditions $\Psi_k = \hat{\Phi}_k = \partial\Psi_k/\partial r = \partial\hat{\Phi}_k/\partial r = 0$ are satisfied on $r=1$ but, in order to perform integration by parts, we need both $\Phi_k^T \Psi_k'/r$ and $\Phi_k^{T'} \Psi_k/r$ to vanish as $r \rightarrow 0$. But Eqs. (30), (31), (36), and (37) establish that $\Phi_k/r \rightarrow 0$ and $\Psi_k/r \rightarrow 0$ as $r \rightarrow 0$, and the derivatives are necessarily finite. Then, from (33) and (35), we find

$$\begin{aligned} \langle \Phi_m, \Psi_n \rangle &= -\frac{1}{\Lambda_n^2} \int_0^1 \frac{1}{r} \Phi_m^T \Psi_n'' dr \\ &= \frac{1}{\Lambda_n^2} \int_0^1 \frac{1}{r} \frac{d\Phi_m^T}{dr} \frac{d\Psi_n}{dr} dr \\ &= -\frac{1}{\Lambda_n^2} \int_0^1 \frac{1}{r} \Phi_m^{T'} \Psi_n dr \\ &= \frac{\Lambda_m^2}{\Lambda_n^2} \langle \Phi_m, \Psi_n \rangle. \end{aligned} \tag{39}$$

But, since the eigenvalues $\{\Lambda_k\}$ are distinct, it follows that

$$\langle \Phi_m, \Psi_n \rangle = Q_n \delta_{nm}. \tag{40}$$

Here δ_{nm} is the usual Kronecker delta and $Q_n = \langle \Phi_n, \Psi_n \rangle$. The quantity Q_n can be easily calculated from (30), (31), (36), and (37) for each eigenvalue Λ_k . Equation (40) is our sought orthogonality condition.

We are now in a position to determine the constants \tilde{B}_k for boundary functions F, G . Substituting the series expression for ψ into (29) we find that, on $z=0$,

$$F = \sum_{k=1}^{\infty} \tilde{B}_k \frac{d\Psi_k}{dr} \Lambda_k^2, \quad G = -\sum_{k=1}^{\infty} \tilde{B}_k \Psi_k / \Lambda_k. \tag{41}$$

But, to apply the binary operator defined above, we need some preliminary manipulation. We differentiate (41a) to obtain the vectorial identity,

$$\left(r \frac{d}{dr} \left(\frac{F}{r} \right) \right) = \sum_{k=1}^{\infty} \tilde{B}_k \Psi_k - \sum_{k=1}^{\infty} \left(1 + \frac{1}{\Lambda_k} \right) \tilde{B}_k \begin{pmatrix} \Psi_k \\ 0 \end{pmatrix}. \tag{42}$$

By applying the operator $\langle \Phi_m, \cdot \rangle$ to both sides, we find

$$\begin{aligned} \tilde{B}_m Q_m - \sum_{k=1}^{\infty} \left(1 + \frac{1}{\Lambda_k} \right) \tilde{B}_k Q_{mk} \\ = \int_0^1 [\hat{\Phi}_m (2(d/dr)(F/r) + G/r) \\ - \Phi_m (d/dr)(F/r)] dr, \end{aligned} \tag{43}$$

where

$$Q_{mk} = \int_0^1 \frac{1}{r} \Phi_m^T \mathbf{M} \begin{pmatrix} \Psi_k \\ 0 \end{pmatrix} dr. \tag{44}$$

Equation (43) represents an infinite set of coupled equations for determining the coefficients \tilde{B}_k . Joseph²² has shown for the problem of the semi-infinite strip that, under certain conditions on the data F, G , the series converges and the solu-

tion is thus ensured. In general, to obtain results from this infinite coupled system in an infinite number of unknowns we will need to resort to series truncation and numerical methods. However, without any further effort we have provided a framework that justifies the approach of the previous sections.

IV. CONCLUSION

The presence of eddies induced in a viscous fluid contained in a stationary semi-infinite cylinder above a rotating end wall when the fluid inertia is significant has been established by Vogel,¹ Escudier,⁵ and Mullin, Kobine, Tavener, and Cliffe.⁷ The current work shows that the eddy structure is present, even when the fluid inertia is very small. The source of the flow character is the complex eigenvalues associated with the homogeneous problem for the first-order inertia correction. Liron and Shahar⁹ and Blake¹¹ have shown that fluid inertia need not be the only source of toroidal eddies.³³ This structure can be induced even in a Stokes flow by the application of a suitable body force. But in these cases too the eddies are traceable to exactly the same complex eigenvalues. It would appear, therefore, that the eddies are an intrinsic feature of the geometry and this speculation is reinforced by experience with the later Re regimes.

The physical setup that we discuss is amenable to experimental investigation. Although the periodicity of the streamfunction of the first-order radial and axial motion is testable, a laboratory setup will be necessarily finite. Due allowance will have to be made for end effects not included in our analysis. We have been concerned with a single cylinder but the analysis of this paper is clearly extendible to the geometry considered by Mullin, Kobine, Tavener, and Cliffe,⁷ when there is an inner coaxial cylinder of constant radius. The boundary conditions on the inner cylinder will lead to the appearance of Bessel functions of the second kind.

ACKNOWLEDGMENTS

It is a pleasure to acknowledge the help and support of my thesis advisor Professor H. K. Moffatt. I would also like to thank Professor T. Mullin for his useful discussion of the cylinder problem and the anonymous referees who brought to my attention Refs. 8, 14, 26, and 27. My work was supported by EPSRC, U.K.

¹H. Vogel, "Experimentelle ergebnisse über die laminare strömung in einem zylindrischen gehäuse mit darin rotierender scheinbe," MPI Bericht 1968, Vol. 6.

²When the fluid inertia is significant, the flow generated in the cylinder by the rotating end wall is found to possess a cellular structure. It is first driven in an outward spiral, as predicted by T. von Karman ["Laminaire und turbulente Reibeng," Z. Angew. Math. Mech. **1**, 233 (1921)], and upon meeting the cylinder wall flows upward until, at a specified height, it moves inward again before being drawn down the center by the pump-like effect of the rotating plate. In experimental systems the cell often encompasses the whole height of the cylinder.

³The term "bubble" is sometimes used to describe the appearance of the small recirculation regions. The terminology has nothing to do with the presence of a cavity in the fluid domain.

⁴M. Bróns, L. Voigt, and J. Sørensen, "Streamline topology of steady axi-

- symmetric vortex breakdown in a cylinder with co- and counter-rotating end-covers," *J. Fluid Mech.* **401**, 275 (1999).
- ⁵M. Escudier, "Observations of the flow produced in a cylindrical container by a rotating end-wall," *Exp. Fluids* **2**, 189 (1984).
- ⁶J. Stevens, J. Lopez, and B. Cantwell, "Oscillatory flow in an enclosed cylinder with a rotating end-wall," *J. Fluid Mech.* **389**, 101 (1999).
- ⁷T. Mullin, J. Kobine, S. Tavener, and K. Cliffe, "On the creation of stagnation points near straight and sloped walls," *Phys. Fluids* **12**, 425 (2000).
- ⁸J. M. Fitz-Gerald, "Plasma motion in narrow capillary flow," *J. Fluid Mech.* **51**, 463 (1972).
- ⁹N. Liron and R. Shahar, "Stokes flow due to a Stokeslet in a pipe," *J. Fluid Mech.* **86**, 727 (1978).
- ¹⁰J. Happel and H. Brenner, *Low Reynolds Number Hydrodynamics* (Prentice-Hall, Englewood Cliffs, 1965).
- ¹¹J. Blake, "On the generation of viscous toroidal eddies in a cylinder," *J. Fluid Mech.* **95**, 209 (1979).
- ¹²The operator \mathcal{D}^2 is intrinsic to the cylindrical geometry and is discussed by Happel and Brenner (Ref. 10).
- ¹³M. Friedmann, J. Gillis, and N. Liron (Ref. 14), in their numerical calculation of the velocity profile of uniform flows entering a pipe, have tabulated the first 30 complex eigenvalues.
- ¹⁴M. Friedmann, J. Gillis, and N. Liron, "Laminar flow in a pipe at low and moderate Reynolds numbers," *Appl. Sci. Res.* **19**, 426 (1968).
- ¹⁵H. K. Moffatt, "The asymptotic behavior of solutions of the Navier-Stokes equations near sharp corners," *Approximate Methods for Navier-Stokes Problems*, in Proceedings of the Symposium held by IUTAM at the University of Paderborn, Germany, 9–15 September 1979, Lecture Notes in Mathematics, edited by R. Rautmann (Springer-Verlag, New York, 1979), Vol. 771, pp. 371–380.
- ¹⁶H. K. Moffatt and B. Duffy, "Local similarity solutions and their limitations," *J. Fluid Mech.* **96**, 299 (1980).
- ¹⁷H. K. Moffatt, "Viscous and resistive eddies near a sharp corner," *J. Fluid Mech.* **18**, 1 (1964).
- ¹⁸C. P. Hills, "Eddy structures induced within a wedge by a circular honing arc," *Theor. Comput. Fluid Dyn.* (in press).
- ¹⁹G. I. Taylor, "On scraping viscous fluid from a plane surface," in *The Scientific Papers of Sir Geoffrey Ingram Taylor*, edited by G. K. Batchelor (Cambridge University Press, Cambridge, 1971), Vol. IV, pp. 410–413.
- ²⁰C. P. Hills and H. K. Moffatt, "Rotary honing: a variant of the Taylor paint-scraper problem," *J. Fluid Mech.* **418**, 119 (2000).
- ²¹R. Smith, "The bending of a semi-infinite strip," *Aust. J. Sci. Res.* **5**, 227 (1952).
- ²²D. Joseph, "The convergence of biorthogonal series for biharmonic and Stokes flow edge problems: Part I," *SIAM (Soc. Ind. Appl. Math.) J. Appl. Math.* **33**, 337 (1977).
- ²³D. Joseph and L. Sturges, "The convergence of biorthogonal series for biharmonic and Stokes flow edge problems: Part II," *SIAM (Soc. Ind. Appl. Math.) J. Appl. Math.* **34**, 7 (1978).
- ²⁴D. Joseph, L. Sturges, and W. Warner, "Convergence of biorthogonal series of biharmonic eigenfunctions by the method of Titchmarsh," *Arch. Ration. Mech. Anal.* **78**, 223 (1982).
- ²⁵C. Liu and D. Joseph, "Stokes flow in wedge-shaped trenches," *J. Fluid Mech.* **80**, 443 (1977).
- ²⁶D. A. Spence, "A class of biharmonic end-strip problems arising in elasticity and Stokes flow," *IMA J. Appl. Math.* **30**, 107 (1983).
- ²⁷J. Harper and G. Wake, "Stokes flow between parallel plates due to a transversely moving end-wall," *IMA J. Appl. Math.* **30**, 141 (1983).
- ²⁸This configuration is sometimes referred to as a "scraping" or "honing" problem due to the implied discontinuity in fluid velocity at the cylinder-plane base contact. A similar situation occurs at the end walls in finite Taylor-Couette geometries and in the Taylor paint-scraper problem [see Taylor (Ref. 19) and Hills and Moffatt (Ref. 20)].
- ²⁹M. Abramovitch and I. Stegun, *Handbook of Mathematical Functions* (Dover, New York, 1965).
- ³⁰Using the well-known recurrence relationships for Bessel functions we could alternatively take a form in terms of J_1 and J'_1 , Y_1 and Y'_1 .
- ³¹We only show $\arg(\Lambda) \in [0, \pi/2]$ since we require the solution to decay and $\Gamma(\bar{\Lambda}) = \overline{\Gamma(\Lambda)}$.
- ³²S. Khuri, "Biorthogonal series solution of Stokes flow problems in sectorial regions," *SIAM (Soc. Ind. Appl. Math.) J. Appl. Math.* **56**, 19 (1996).
- ³³Although the eddies of this paper and of the earlier works of Liron and Shahar (Ref. 9) and Blake (Ref. 11) are all attributable to complex eigenvalues, it is perhaps worth emphasizing the fundamental difference between these studies. In the earlier works the toroidal eddies arose due to the Stokeslet forcing at the level of the zeroth-order (Stokes) flow. For the rotating end-wall configuration the zeroth-order flow is purely azimuthal and the toroidal eddies are induced by the effects of the small inertia correction.